JCTC Journal of Chemical Theory and Computation

Article

pubs.acs.org/JCTC

Dispersion- and Exchange-Corrected Density Functional Theory for Sodium Ion Hydration

Marielle Soniat,[†] David M. Rogers,[‡,¶] and Susan B. Rempe*[,‡]

[†]Department of Chemistry, University of New Orleans, 2000 Lakeshore Drive, New Orleans, Louisiana 70148, United States

[‡]Center for Biological and Engineering Sciences, Sandia National Laboratories, Albuquerque, New Mexico 87123, United States

[¶]Department of Chemistry, University of South Florida, Tampa, Florida 33620, United States

Supporting Information

ABSTRACT: A challenge in density functional theory is developing functionals that simultaneously describe intermolecular electron correlation and electron delocalization. Recent exchange-correlation functionals address those two issues by adding corrections important at long ranges: an atom-centered pairwise dispersion term to account for correlation and a modified long-range component of the electron exchange term to correct for delocalization. Here we investigate how those corrections influence the accuracy of binding free energy predictions for sodium-water clusters. We find that the dual-corrected ωB97X-D functional gives cluster binding energies closest to high-level *ab initio* methods (CCSD(T)). Binding energy decomposition shows that the ωB97X-D functional predicts the smallest ion−water (pairwise) interaction energy and larger multibody contributions for a four-water cluster than most other functionals − a trend consistent with CCSD(T) results. Also, ωB97X-D produces the smallest amounts of charge transfer and the least polarizable waters of the density functionals studied, which mimics the lower polarizability of CCSD. When compared with experimental binding free energies, however, the exchange-corrected CAM-B3LYP functional performs best (error <1 kcal/mol), possibly because of its parametrization to experimental formation enthalpies. For clusters containing more than four waters, "split-shell" coordination must be considered to obtain accurate free energies in comparison with experiment.

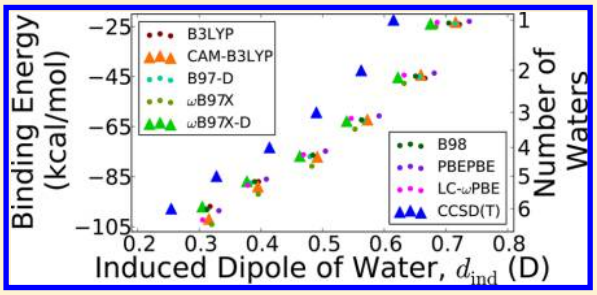

1. INTRODUCTION

Systems with both ionic and dispersive interactions are important and ubiquitous in chemistry and biology. For example, the free energies of ion solvation relative to protein binding determine equilibrium selectivity in transmembrane ion channel proteins.[1−4] Dispersive contributions to ionic binding are expected to be small,[5,6] but may be necessary to obtain chemical accuracy in binding free energies. Because of its computational efficiency, density functional theory (DFT) is desirable for electronic structure computations for large systems. Though the Hohenberg−Kohn theorem states that an exact density functional (DF) would predict the exact electron density and associated energy,[7,8] the approximate methods currently in use do not yet fulfill this ideal. DFT is especially inadequate for binding in dispersion-dominated systems, underestimating the binding energy in noncovalent molecular pairs by as much as 85% in extreme cases.[9]

Dispersion forces arise from fluctuations in electron distributions and can be described by dynamical correlation between electrons. Those electron correlations give rise to the van der Waals (vdW) attraction between molecules.[10] The leading term of the vdW attraction decays as $1/r^6$, where r is the intermolecular distance. Though weak compared to electrostatics, dispersion is vital in the study of liquid water[11−13] and water clusters.[14]

An important question is whether intermolecular dispersion contributes significantly to selective ion solvation, where electrostatic interactions might otherwise be expected to dominate. An interesting test case pertinent to ion channels[15] in cellular membranes involves sodium ion (Na^+) solvated by water molecules (H_2O). Water−water interactions in ion−water clusters (6−10 Å in diameter) fall in the distance region critical for describing the transition from local to nonlocal dispersive effects.[16] Here, that distance is termed long-ranged even though it applies to intermolecular distances that may be within a couple Ångstroms.

The standard method for electronic structure calculations, Hartree−Fock (HF) theory, excludes electron correlations but treats electrostatic (Coulomb) and electron exchange exactly at all distances. The "gold standard" for noncovalent interactions is the post-HF coupled cluster method with single, double, and perturbative triple excitations (CCSD(T)) at the complete basis set limit. Coupled cluster methods account for electron correlation by including mixtures of multiply excited single-electron states that lower the Hartree−Fock (self-consistent field) ground-state energy, thereby defining one measure of dispersive attraction. Since the perturbative triples calculation

Received: December 8, 2014
Published: June 5, 2015

DOI: 10.1021/acs.jctc.5b00357
J. Chem. Theory Comput. 2015, 11, 2958−2967

scales as the seventh power of the basis set size, it quickly becomes intractable for large systems.[17] DFT is popular because it is more accurate than HF yet less computationally expensive than post-HF methods like CCSD(T).[18]

The purpose of this study is to determine the DF that best describes binding in small sodium-water clusters ($Na^+\cdot(H_2O)_n$ up to $n = 6$ waters). In the process, we will assess whether dispersion, or other long-ranged corrections, are necessary in these ionic systems. The DFs studied herein fall into five categories:

(i) a generalized gradient approximation [GGA] (PBEPBE),
(ii) hybrid GGAs (B98, B3LYP),
(iii) a dispersion-corrected hybrid GGA (B97-D),
(iv) range-separated GGAs (LC-ωPBE, CAM-B3LYP, ωB97X),
(v) a combination of range separation and dispersion correction (ωB97X-D).

These density functionals cover a range of approaches for correcting the deficiencies of DFT in describing dispersion interactions. For a more thorough description of GGAs and hybrid DFs, see the Supporting Information or reviews by Burke and co-workers[19,20] and Cohen, Mori-Sanchez, and Yang.[7]

In the DFT-D approach to correcting density functionals (category (iii) above), a simple sum of van der Waals interactions between atomic pairs is added to the total energy. Then the dispersion correction takes the form $E_{disp} = \sum_{i<j} - C_6^{ij}/r_{ij}^6$, where r_{ij} represents the distances between atomic pairs. The dispersion coefficients (C_6) are determined for each atom type and combined geometrically for each atomic pair. Grimme[21] found that adding dispersion corrections improves accuracy compared to any DF without long-ranged corrections. However, Grimme's comparison is for the S22 benchmark set of dimer interaction energies,[22] which does not include ions. The strongly polarizing environment around a cation can cause electron delocalization from a ligating water onto the ion,[23] which may in turn reduce dispersive water−water interactions (i.e., alter C_6^{ij}).

While DFT-D concentrates specifically on dispersion to account for electron correlation at intermolecular distances, range separation focuses on the exchange term to correct the electron delocalization error in DFT functionals.[24−28] Long-range corrected (LC) functionals transition from DFT exchange at short distances to pure HF exchange at long-range. Such a transition prevents HF exchange from interfering with the short-range properties of the density functional, while capturing the correct exchange at long distances. The Coulomb-attenuating method (CAM) differs from other LC functionals by keeping some DFT exchange at long-range.[29] When used as a reference state for symmetry-adapted perturbation theory on the S22 and S66 data sets, wave functions from range-separated DFT methods yield most energy components in remarkable agreement with high-level *ab initio* methods.[30] This agreement depends on choosing the range separation distance to be consistent with the molecular ionization potential.

Since neither distance-dependent exchange-correlation functionals nor HF explicitly include dispersion, the long-range dispersion term must be added. Some functionals have been reparameterized to include both LC and DFT-D corrections, such as ωB97X-D.[31] Other dual-corrected functionals exist as well.[32,33] Those functionals show some promise for addressing multibody effects due to collective induced-dipole interactions.[31−33]

In the work presented here, we compare DFT results on Na^+-water binding to both high-level *ab initio* (CCSD(T)) calculations and experiment. We find that the extent of water electronic polarization, measured as induced water dipoles, captures the major differences between the functionals tested. The density functionals predict stronger binding energies compared to CCSD(T) due mainly to stronger polarization of the electronic structure. Stronger multibody interactions in the DFs relative to CCSD(T) also contribute to more favorable binding energies. Neither dispersion nor range corrections alone improves the DF energy predictions.

The most accurate DF for electronic binding energy found in the current study, ωB97X-D, contains corrections for both dispersion and range separation. That dual-corrected functional also agrees well with CCSD in free energy and the dipole moments of waters complexed with Na^+. While all density functionals predict binding free energies that fall within experimental error, the range-corrected CAM-B3LYP functional agrees best with experiment. All DFs show that split-shell coordination is favorable beyond $n = 4$ waters at both $T = 0$ K and $T = 298$ K.

2. METHODS

The DFs under study are B3LYP,[34−37] CAM-B3LYP,[29] B97-D,[38] ωB97X,[39] ωB97X-D,[31] B98,[40,41] PBEPBE (PBE form for both exchange and correlation functionals),[42,43] and LC-ωPBE.[44−46] Supplementary Tables S1 and S2 give further details on the adjustable parameters and training sets used in these DFs.

2.1. Electronic Energy. Our first goal is to compare binding energies across the density functionals (DFs), listed above, for the same cluster conformation. Binding energy calculations are performed for the series of sodium (Na^+) clustering reactions with n water molecules (H_2O)

$$Na^+ + n(H_2O) \leftrightarrow Na^+\cdot(H_2O)_n \quad (1)$$

Lowest-energy structures are found for a single water molecule and for sodium-water clusters ($Na^+\cdot(H_2O)_n$, $n = 1-6$) using CCSD/6-31++G**.[47−51] Single-point energy calculations are performed on those CCSD-optimized structures using CCSD, CCSD(T), and DFT with a correlation consistent triple-ζ basis set on all atoms (aug-cc-pVTZ).

The binding energy for formation of a cluster with n waters is calculated as

$$\Delta E_n = E_{[Na(H_2O)_n]^+} - E_{Na^+} - nE_{H_2O} \quad (2)$$

where $E_{[Na(H_2O)_n]^+}$ is the total energy of the cluster, E_{Na^+} is the energy of the lone sodium ion, and E_{H_2O} is the energy of a lone water molecule. The binding energies are calculated at temperature $T = 0$ K and do not include corrections for basis set superposition errors. The binding energies of CCSD/aug-cc-pVDZ are converged with respect to basis set size (within 1 kcal/mol of aug-cc-pVTZ), as is the magnitude of the basis set superposition error (BSSE). Binding energies with MP2/aug-cc-pVDZ agree to within 0.2 kcal/mol of CCSD energies using the same basis.

2.2. Electrostatic Properties. Our second goal is to evaluate electrostatic properties because electrostatic interactions dominate ion−water binding energies. Specifically, we compute the correlation of the binding energy with two

DOI: 10.1021/acs.jctc.5b00357
J. Chem. Theory Comput. 2015, 11, 2958−2967

properties: (i) the average charge transfer from each water in the cluster to sodium, q_{CT}/n, and (ii) the average induced dipole moment of each water in the cluster, d_{ind}.

Atomic partial charges (q_a) and atomic dipoles ($\vec{d}_a$) are found using the quantum theory of atoms in molecules, which decomposes electron density into basins around each atom.[52] The basin boundaries are determined using electron density, as implemented in MultiWfn.[53] Because the basin centers of electron density, $\vec{y}_a$, are slightly shifted from the atom centers, $\vec{x}_a$, the difference is added to each atomic dipole using $\vec{d}_a = \vec{p}_a + (q_a - Z_a)(\vec{y}_a - \vec{x}_a)$, where $\vec{p}_a$ is the basin electron dipole moment, Z_a is the nuclear charge, and $q_a - Z_a$ is the integral of the electron density in the basin belonging to atom 'a'.

From the atomic charges, dipoles, and positions, the average induced dipole moment of water (d_{ind}), projected along the direction from sodium to the water ('w') center of mass ($\vec{x}_w^{cm}$), is calculated by

$$d_{ind} = \frac{1}{n}\sum_{w=1}^{n} \mathrm{Proj}_{\vec{x}_{Na^+}\to\vec{x}_w^{cm}}\left(\sum_{a\in w} \Delta q_a \vec{x}_a + \Delta\vec{d}_a\right) \quad (3)$$

The average amount of charge transferred from each water in the cluster to Na^+ (q_{CT}/n) is given by the calculated atomic charge on Na^+ (q_{Na}) relative to the +1 charge of the isolated ion

$$q_{CT}/n = (1 - q_{Na})/n \quad (4)$$

The Δ symbols in eq 3 indicate differences with respect to the lone water molecule, calculated using a single geometry and with a DFT (or CCSD) method matching that used for the cluster. The reference water geometry is found by optimizing the electronic energy using CCSD with the 6-31++G** basis set, followed by charge and dipole calculations using the aug-cc-pVDZ basis set. The calculations were repeated using a water geometry optimized with CAM-B3LYP and 6-31++G** (not shown). Because the optimized water geometries are so alike, there is no distinguishable change in any of the results other than a shift of the dipole for the reference water in the direction of the hydrogens by an extra 0.018 D.

2.3. Electronic Binding Energy Decomposition. A third interest is how dispersion and range corrections affect multibody interactions. To this end, an energy decomposition is performed for the $n = 4$ cluster in the CCSD-optimized geometry. The pairwise terms consist of the ion−water (E_{iw}) and water−water (E_{ww}) interactions. The three-body terms include the ion−water−water (E_{iww}) and water−water−water (E_{www}) interactions. To third order, the binding energy of $Na^+\cdot(H_2O)_4$ is

$$\Delta E^{(3)} = 4(\langle E_{iw}\rangle + \langle E_{www}\rangle) + 6(\langle E_{ww}\rangle + \langle E_{iww}\rangle) \quad (5)$$

The remaining (fourth-order and higher) terms are equal to the total binding energy minus the third-order binding energy

$$\text{Remainder} = \Delta E - \Delta E^{(3)} \quad (6)$$

2.4. Thermochemistry. The fourth goal is to evaluate each DF's performance for thermochemical calculations. For these calculations, the structure must be at a minimum on the potential energy surface for that particular DF. Therefore, cluster and water structures are reoptimized for each DF and for CCSD with the aug-cc-pVDZ basis set. The clusters include $n = 1-6$ waters for the DF calculations and $n = 1-4$ waters for CCSD, due to computational expense. Tight convergence criteria for geometry optimization are used to ensure reliable low-frequency vibrational modes are found. No correction is applied for basis set superposition error since ΔE_n predictions indicate that none are needed. Convergence is reached when the total DFT density matrix has a root-mean-square difference of $<10^{-8}$ between iterations.

Vibrational frequency analysis using an extra fine integration grid is performed to obtain thermal corrections to the energy at temperature $T = 298$ K. All vibrational frequencies are positive, indicating that the optimized cluster configurations represent minimum-energy structures. The binding enthalpies, $\Delta H°$, are calculated by

$$\Delta H_n°(298\text{ K}) = (E + H_{corr})_{[Na(H_2O)_n]^+} - (E + H_{corr})_{Na^+} - n(E + H_{corr})_{H_2O} \quad (7)$$

Similarly, the binding free energies, $\Delta G°$, are

$$\Delta G_n°(298\text{ K}) = (E + G_{corr})_{[Na(H_2O)_n]^+} - (E + G_{corr})_{Na^+} - n(E + G_{corr})_{H_2O} \quad (8)$$

where E is the total electronic energy of each cluster or monomer. The thermal corrections for the enthalpy and free energy (H_{corr} and G_{corr}) are computed from the rigid-rotor harmonic oscillator approximation to the translational, rotational, and vibrational nuclear Hamiltonians.[54−56] Those corrections allow for direct comparison to experiment at finite temperatures and influence the stability (free energy) of the different coordination structures.[57]

Experimental values for binding enthalpies and free energies are taken from Tissandier et al.,[58] which gives a compilation of data from the Kebarle[59] and Castleman research groups.[60] Error bars for the experimental data are not reported, but from the analysis of Tissandier, it appears an experimental error of 10−15% is reasonable. Frequency scaling is not used in the calculations.

Only harmonic frequencies[61] are calculated due to the computational expense of anharmonic calculations. Previous work compared binding free energies for one ion relative to another. That work reported that harmonic frequencies are sufficient for $n \leq 4$, with anharmonic effects becoming important only for larger clusters.[62,63] Nevertheless, vibrational modes in individual clusters may include low-frequency hindered rotations that may be treated more accurately with an anharmonic potential model or path-integral methods.[64] Thus, a hindered rotor correction for water rotation about the metal−oxygen bond was considered as well for the $n = 4$ cluster.[65,66] Since that correction contributes less than 1 kcal/mol to the entropy, it is neglected in the final free energy calculations. Calculations are done using NWChem (version 6.1)[67−69] and Gaussian09[70] electronic structure software packages.

2.5. Error Reporting. The error is reported as mean absolute error (MAE) of the sequential water binding energy

$$\mathrm{MAE}(n_{max}) = \frac{1}{n_{max}}\sum_{n=1}^{n_{max}} |\Delta E_n^{calc.} - \Delta E_n^{Tiss.}| \quad (9)$$

where $\Delta E_n^{calc.}$ is the calculated binding energy, enthalpy, or free energy, and $\Delta E^{Tiss.}$ is the corresponding experimental value compiled in Tissandier et al.[58] For comparison of binding energies (ΔE_n), the calculated energies are compared with CCSD(T) energies, and thus $\Delta E^{Tiss.}$ is replaced with ΔE^{CCSD} in

DOI: 10.1021/acs.jctc.5b00357
J. Chem. Theory Comput. 2015, 11, 2958−2967

eq 9. The MAE(4) and MAE(6) are considered separately because of the greater uncertainty in the n = 5−6 structures.

3. RESULTS

3.1. *Ab Initio* Benchmarking: Electronic Binding Energy. Electronic binding energy (ΔE_n) is computed for identical $Na^+\cdot(H_2O)_n$ structures. The coupled cluster CCSD(T) method provides a standard for evaluating the predictions of exchange-correlation functionals. All calculations use the aug-cc-pVTZ basis set.

Adding water to Na^+ in gas phase is always favorable in terms of electronic binding energy (Figure 1). The change in electronic energy (ΔE) is the largest component of the $Na^+\cdot(H_2O)_n$ cluster formation free energies ($\Delta G°$).

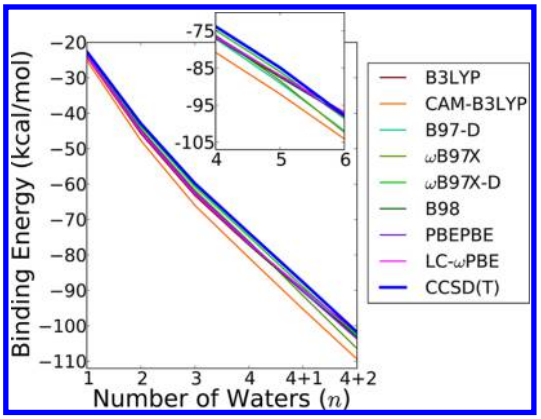

Figure 1. Binding energy (ΔE_n) for formation of sodium-water clusters, including split-shell structures for 5-fold (n = 4 + 1) and 6-fold (n = 4 + 2) clusters. The inset shows only inner-shell $Na^+\cdot(H_2O)_n$ structures. The same geometry is used for each method (see text). ωB97X-D best matches the CCSD(T) results. Tabulated values appear in Supplementary Table S5.

The mean absolute error (MAE) of binding energy compared to CCSD(T)/aug-cc-pVTZ is calculated for two subsets of clusters: from n = 1 to n_{max} = 4 and from n = 1 to n_{max} = 6 (Table 1). For the subset identified as n_{max} = 6, the MAE is calculated separately for inner-shell (is) and split-shell (ss) structures. In inner-shell structures, all waters coordinate directly with the ion. In split-shell structures, denoted as $n = n_i + n_o$, some (n_o) waters move away from the ion to form a second solvation shell outside the inner-shell (n_i) waters. The MAE are shown separately in anticipation of two sources of uncertainty in the thermochemical calculations. First, the experimental configurations at n = 5 and 6 are uncertain. Second, errors may arise at higher coordination due to the approximation of harmonic vibrational frequencies. Illustration of these structures appears in Figure 2.

Table 1. Mean Absolute Error (MAE), As Defined in Eq 9, in Electronic Binding Energy (ΔE_n) Compared to CCSD(T) Using the aug-cc-pVTZ Basis, with Standard Deviation in Parentheses[a]

	MAE(4)	MAE(6,is)	MAE(6,ss)
B3LYP	3 (1)	3 (1)	3 (1)
CAM-B3LYP	6 (2)	6 (2)	6 (2)
B97-D	2 (1)	3 (1)	2 (1)
ωB97X	2 (1)	3 (1)	3 (1)
ωB97X-D	1 (0.4)	1 (0.4)	1 (0.3)
B98	3 (1)	2 (1)	3 (1)
PBEPBE	2 (1)	2 (1)	2 (1)
LC-ωPBE	3 (1)	2 (1)	2 (1)
CCSD	0.4 (0.1)	0.4 (0.2)	0.4 (0.2)

[a]The set of structures analyzed for n_{max} = 4 and n_{max} = 6 inner-shell (is) or split-shell (ss) coordinations represent the lowest-energy configurations for CCSD/6-31++G**. Units are kcal/mol.

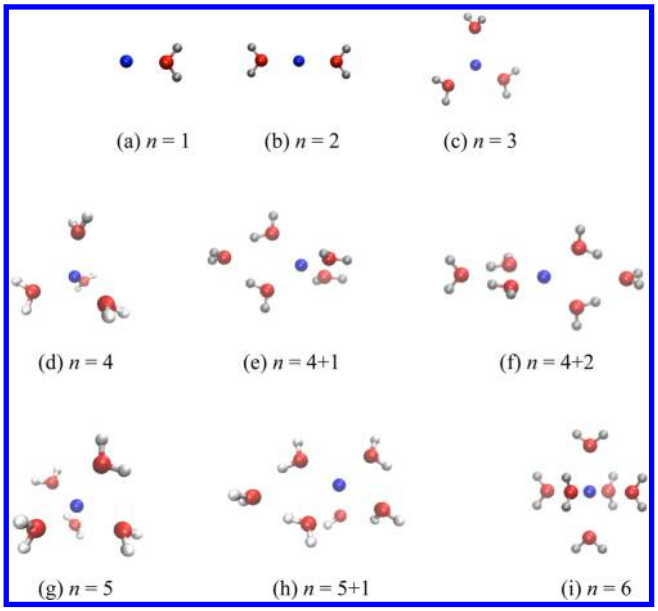

Figure 2. Geometries of sodium-water clusters, $Na^+\cdot(H_2O)_n$.

Of all the density functionals, the ωB97X-D exchange-correlation functional gives results closest to CCSD(T) for electronic binding energy (ΔE_n). Although it averages 1.2 kcal/mol (2% error) lower in binding energy than CCSD(T), ωB97X-D shows a remarkable precision of 0.4 kcal/mol across all n. CAM-B3LYP produces results furthest from CCSD(T), with binding energy up to 12% lower. Interestingly, the split-shell coordination is favored for all methods for clusters with $n \geq 5$ waters, even at T = 0 K. This trend contrasts with previous works,[57,71−74] in which inner-shell coordination is favored at T = 0 K.

A systematic error appears in the DFs compared to CCSD(T). All the density functionals show more favorable binding than CCSD(T), by 1 to 6 kcal/mol (Table 1). To investigate whether this difference is related to polarization of electron distributions in the ion−water clusters, the binding energy is compared to induced dipoles (d_{ind}) on the water molecules and charge transfer (q_{CT}/n) between waters and the ion for the inner-shell n = 1−6 clusters.

3.2. Electrostatic Properties. Strong correlations are apparent between binding energies and key electrostatic properties (Figure 3). As the cluster size increases from n = 1 to 6, the cluster formation energy (ΔE_n) becomes progressively more favorable. At the same time, both the average charge transferred from each water to the Na^+ ion (q_{CT}/n, Figure 3a) and the water dipole induced by Na^+ binding (d_{ind}, Figure 3b) decrease almost linearly toward zero (linear correlation coefficients of r = 0.92 and 0.96). Despite the weaker charge transfer per water with increasing cluster size, the net effect of each added water continues to reduce the positive charge on Na^+ so that the Na^+ partial charge (q_{Na}) is

DOI: 10.1021/acs.jctc.5b00357
J. Chem. Theory Comput. 2015, 11, 2958−2967

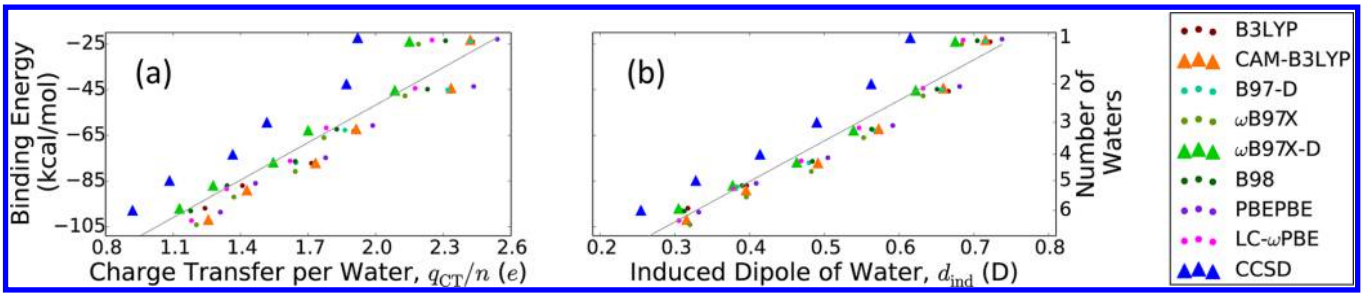

Figure 3. Cluster binding energy (ΔE_n) is correlated with (a) the charge transferred to sodium per water molecule, $q_{CT}(Na)/n$ (r = 0.92) in units of elementary charge 10^{-2} e, and (b) the average induced dipole of the water molecules, d_{ind} (r = 0.96) in units of Debye. Here, r is the linear correlation coefficient, computed for n = 1−6. Note that the number of waters increases from top to bottom. Symbols for the DFs of interest, CAM-B3LYP and ωB97X-D, and CCSD are enlarged for emphasis. Charge transfer and induced water dipoles are smallest for CCSD. Of the DFs, charge transfer and induced dipoles are smallest for ωB97X-D and largest for PBEPBE. CAM-B3LYP, which predicts the most favorable binding energies, also has relatively large charge transfer and induced water dipoles.

also correlated with the cluster binding energy, with a linear correlation coefficient of r = 0.95 (not shown).

The basin decomposition analysis (section 2.2) also allows us to separate the induced dipole (eq 3) into contributions from atomic charges and geometry ($q_a\vec{x}_a$) and from the atomic dipole moments ($\vec{d}_a$). Because the cluster and reference water geometries ($\vec{x}_a$) are fixed in this part of the analysis, the component of the induced dipole due to the charge represents a charge flow polarizability.[10] The correlation between binding energy and the total induced dipole (r = 0.96) is nearly identical to that between the binding energy and the separate charge (r = 0.95) and atomic dipole (r = 0.96) components. Each contributes roughly half to the total induced dipole of each water (57% from the charge and 43% from the dipole component).

The charge transfer (q_{CT}/n) and induced water dipoles (d_{ind}) are smaller for CCSD than for any of the DFs. The ωB97X-D exchange-correlation functional shows the smallest charge transfer amounts and smallest induced water dipoles relative to CCSD, as well as the closest agreement to the CCSD(T) binding energies (Figure 1, Table 1). The higher, less favorable binding energies (ΔE_n) typically found for ωB97X-D are consistent with reduced water charge transfer and induced dipole moments compared with the other DFs. The strong correlation found here implies that electronic polarization accounts for a large part of the differences in DF binding energies.

DFs are known for overpolarizability of electron distributions arising from issues with accommodating the discrete, antisymmetric nature of the wave function with respect to electron exchange in density functional methods.[24−28,75] This issue is known as the density-driven electron delocalization or electron self-interaction error. The influence of electronic polarization on binding energy supports the use of charged and highly polarized systems alongside traditional noncovalent systems for DF parametrization, as demonstrated in the parametrization of ωB97X-D.[39]

3.3. Electronic Binding Energy Decomposition. To study the contributions of multibody interactions to the total binding energy, an energy decomposition (see eqs 5 and 6) is performed for the n = 4 cluster in the CCSD-optimized geometry. The results are presented in Table 2. CCSD results agree with CCSD(T).

On average, the third-order binding energy is 5.6 kcal/mol lower (more favorable) than the total binding energy for the DFs and 8.4 kcal/mol lower than the total CCSD binding energy, reported as "remainder" in Table 2. These values are equivalent to ≈7% and ≈11% of the total binding energy for DFT and CCSD, respectively. Such a large discrepancy indicates that fourth-order and higher terms in the binding energy are important in cation-water clusters and act to destabilize the clusters. This destabilization is in contrast with the favorable contribution found for higher-order multibody contributions (without electrostatic embedding) in the $(H_2O)_6$ and $(H_2O)_6{\cdot}F^-$clusters.[76] Rather than helping cancel uncorrected BSSE as rationalized in that work, relying on the third-order cluster energy would exacerbate any basis set error in $(H_2O)_6{\cdot}Na^+$. The difference in fourth-order and higher terms for DFs and CCSD may reflect the parametrization of DFs, which concentrates on single-molecule properties and dimer interactions.

Table 2. Decomposition of the Binding Energy of the $Na^+{\cdot}(H_2O)_4$ Cluster[a]

method	$\langle E_{iw}\rangle$	$\langle E_{ww}\rangle$	$\langle E_{iww}\rangle$	$\langle E_{www}\rangle$	remainder	total ΔE
B3LYP	−25.2	1.6	1.5	−0.2	5.8	−77.2
CAM-B3LYP	−26.1	1.6	1.6	−0.1	4.8	−80.8
B97-D	−24.8	1.3	1.6	−0.1	5.1	−77.1
ωB97X	−24.7	1.5	1.4	−0.1	5.6	−76.2
ωB97X-D	−24.4	1.5	1.4	−0.1	5.8	−74.8
B98	−25.0	1.4	1.6	−0.1	5.4	−77.0
PBEPBE	−24.8	1.3	1.7	−0.1	5.2	−76.4
LC-ωPBE	−25.2	1.6	1.5	−0.2	6.2	−76.8
CCSD	−24.4	1.3	1.4	−0.1	8.5	−73.8
CCSD(T)	−24.2	1.2	1.4	−0.1	8.3	−73.3

[a]The binding energy to third order, $\Delta E^{(3)}$, is defined in eq 5. The remainder is defined in eq 6. Units are in kcal/mol.

As expected, the pairwise ion−water interactions provide the dominant contribution to the binding energy and stabilize the structure. In contrast, water−water pairwise interactions destabilize the cluster and contribute only ≈12% to the total binding energy. Such ligand−ligand repulsion has been observed for water previously[23,77−79] and is related to the decrease in water dipole when additional waters coordinate the cation.[23,77] The largest nonpairwise interaction comes from ion−water−water interactions, which also destabilize cluster formation by an additional ≈12% of the total energy. All the DFs overestimate the ion−water term compared to CCSD. This term is also the largest source of differences between the DFs. Such overly strong binding is related to the overpolarization issue discussed above. DFT's tendency to smear

DOI: 10.1021/acs.jctc.5b00357
J. Chem. Theory Comput. 2015, 11, 2958−2967

out the electron distribution leads to larger induced dipoles than CCSD, which in turn contribute to overbinding.

The dispersion correction adds a favorable contribution to the total binding energy. Interestingly, switching from ωB97X to the dispersion-corrected ωB97X-D raises the ion−water binding energy. A less favorable binding energy in this case must be due to the only other difference between those two functionals besides the dispersion correction − the increased amount of HF exchange at short-range and decreased amount at long-range in ωB97X-D compared to ωB97X.[16] The slight decrease in ion−water interaction strength mirrors the same decrease that appears when adding the triples correction to CCSD.

In general, an overly favorable dispersion correction moves the energy further away from high-level *ab initio* results for small ion−water systems. As an example, the pairwise dispersion correction is calculated for B97-D in the $Na^+\cdot(H_2O)_4$ geometry, using the stand-alone DFT-D3 software.[80] Dispersion contributes −1.6 kcal/mol to $\langle E_{iw}\rangle$ and 0.1 kcal/mol to $\langle E_{ww}\rangle$, which corresponds to ≈6% for both $\langle E_{iw}\rangle$ and $\langle E_{ww}\rangle$. In the DFT-D2 scheme, with which B97-D is parametrized, the C_6 terms are independent of coordination state, and the damping parameters were set *a priori*.[38] The improvements made in the DFT-D3 scheme reduce the dispersion correction in $\langle E_{iw}\rangle$ to −0.9 kcal/mol for a single ion−water interaction. This removes some of the overly favorable binding energy, increasing it by ≈3 kcal/mol for the case of n = 4 waters.

The ωB97X-D exchange-correlation functional stands out from the other DF. That functional consistently shows the lowest electronic polarization for $Na^+\cdot(H_2O)_n$ clusters (section 3.1). Reduced polarization corresponds to less electrostatic (Coulomb) attraction. The ωB97X-D compensates for the smaller electrostatic term with an attractive dispersion term. Furthermore, the unfavorable high-order multibody terms in the binding energy are closer to CCSD values than most other functionals (Table 2). The result is a density functional that agrees well with CCSD/CCSD(T) for ion binding energies of identical Na^+-water clusters when a combination of both range separation and dispersion correction is included.

3.4. Experimental Benchmarking: Binding Enthalpy and Free Energy. Calculation of enthalpies and free energies permits direct comparison to experiments on single-ion hydration. Geometry optimization and frequency calculations are performed for each $Na^+\cdot(H_2O)_n$ cluster using each DF and CCSD with the aug-cc-pVDZ basis set. Strict convergence criteria (see Methods) are used to ensure a true minimum on the potential energy surface is reached. Results are evaluated for convergence with respect to basis set size by repeating the optimization and frequency calculations with aug-cc-pVTZ. All DFs are well-converged with the double-ζ basis set since there is ≤1 kcal/mol difference between the binding free energies calculated at the double- and triple-ζ levels.

For $n \leq 4$, the lowest free energy structures have all waters directly coordinated to the ion. For five and six waters, split-shell coordinations of n = 4 + 1 and n = 4 + 2 give structures with the lowest free energy at T = 298 K (Figure 2). Structural details are given in the Supporting Information. The structures with the lowest free energy for the sodium-water association reactions of eq 1 should be the experimentally relevant structures. The enthalpy and free energy of the most stable structures (in terms of free energy) are shown in the main plots of Figures 4 and 5. The figures' insets show results for the inner-shell structures and the split-shell n = 5 + 1 structure.

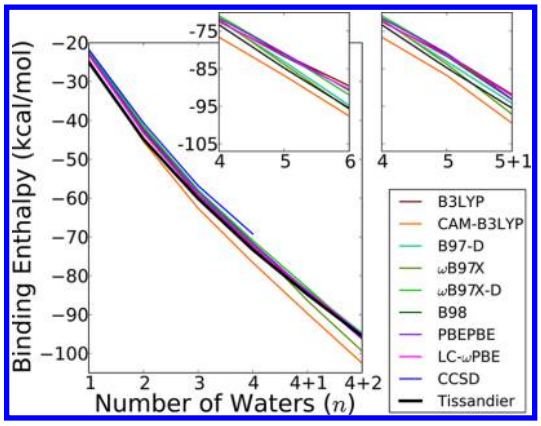

Figure 4. Binding enthalpy (ΔH_n°) for formation of sodium-water clusters, including split-shell structures for 5-fold (n = 4 + 1) and 6-fold (n = 4 + 2) complexes. The left inset shows only inner-shell structures, and the right inset shows the 6-fold split-shell structure, n = 5 + 1. Tabulated values appear in Supplementary Table S6.

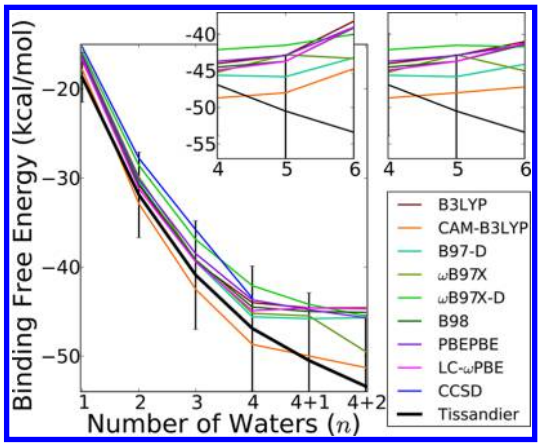

Figure 5. Binding free energy (ΔG_n°) for formation of sodium-water clusters, including split-shell structures for 5-fold (n = 4 + 1) and 6-fold (n = 4 + 2) complexes. The left inset shows only inner-shell structures, and the right inset shows the 6-fold split-shell structure, n = 5 + 1. Only the split-shell structures have the correct trend in binding free energy. The error bars show ±15% of experimental values. Tabulated values appear in Supplementary Table S7.

Adding water to Na^+ in gas phase is always favorable in terms of energy and binding enthalpy (Figures 1 and 4). As water adds to the second shell of solvent molecules (n = 4 + 1, n = 4 + 2), the slope of the binding free energy curve starts to level off (Figure 5). With enough waters, the binding free energy would approach the constant value for Na^+ solvation in bulk liquid water. In contrast, waters added to the inner shell result in less favorable binding free energy for n > 4, as expected when crowding causes repulsion between coordinated ligands.[23,77,78] No more than n = 6 waters can be added to the inner hydration shell of Na^+, which is consistent with earlier results found for Na^+.[81−85]

Errors are not reported in the original experimental works.[60,86] If we assume that errors of 10−15% are reasonable, then all the DF and CCSD predictions fall within the experimental error bars for enthalpy. For free energy, the DFs are within error bars of experiment up to n = 4 + 1. At n = 4 + 2, only half of the DFs are within 15% of experimental values. Although other reports suggest that long-range-corrected functionals produce increased errors in vibrational

DOI: 10.1021/acs.jctc.5b00357
J. Chem. Theory Comput. 2015, 11, 2958−2967

frequencies,[87] we do not see significant degradation in thermochemical properties using those functionals.

In the calculation of binding enthalpy ($\Delta H°$), all the functionals give results within ±3 kcal/mol of experimental values reported in Tissandier et al.[58] For the most part, the differences between the DFs are insignificant. The MAE with respect to experiment and CCSD are reported in Table 3.

Table 3. Mean Absolute Error (MAE) in Enthalpy ($\Delta H°$), As Defined in Eq 9, Compared to CCSD and Experiment with aug-cc-pVDZ, with Standard Deviation in Parentheses[a]

		Tissandier	
	CCSD MAE(4)	MAE(4)	MAE(6,ss)
B3LYP	3 (1)	1 (1)	1 (1)
CAM-B3LYP	5 (2)	2 (1)	3 (2)
B97-D	2 (1)	2 (1)	2 (1)
ωB97X	2 (1)	2 (1)	2 (1)
ωB97X-D	1 (1)	3 (1)	2 (1)
B98	2 (1)	2 (1)	1 (1)
PBEPBE	2 (1)	2 (0.4)	2 (1)
LC-ωPBE	2 (1)	1 (1)	1 (1)
CCSD		4 (0.5)	

[a]Units are kcal/mol.

B3LYP, B98, and LC-ωPBE give binding enthalpy results closest to experimental values over the range of coordination numbers. ωB97X-D predicts $\Delta H°$ closest to CCSD, but both are farthest from experimental values. Binding enthalpies tend to be lower for the split-shell structures, though not necessarily closer to the experimental values.

The binding free energy predictions (ΔG_n°) differ more from experiment than the same comparison with binding enthalpy (Table 4). Accuracy relative to experiment decreases sharply for

Table 4. Mean Absolute Error (MAE) in Free Energy ($\Delta G°$), As Defined in Eq 9, Compared to CCSD and Experiment with aug-cc-pVDZ, with Standard Deviation in Parentheses[a]

		Tissandier	
	CCSD MAE(4)	MAE(4)	MAE(6,ss)
B3LYP	2 (1)	2 (1)	4 (3)
CAM-B3LYP	5 (2)	1 (0.4)	1 (1)
B97-D	2 (1)	2 (1)	3 (3)
ωB97X	2 (1)	2 (0.4)	3 (1)
ωB97X-D	1 (0.4)	4 (1)	5 (2)
B98	2 (1)	2 (1)	4 (3)
PBEPBE	2 (1)	2 (1)	4 (2)
LC-ωPBE	2 (1)	2 (1)	3 (3)
CCSD		4 (1)	

[a]Units are kcal/mol.

$n > 4$. The binding free energy curves for inner-shell structures $n = 5 + 0$ and $n = 6 + 0$ disagree even qualitatively with experiment. Only when split-shell configurations are considered do the qualitatively correct trends appear (Figure 5). Again, there is not a significant difference between most of the tested DFs with respect to the MAE. However, only CAM-B3LYP with split-shell coordination achieves chemical accuracy of ±1 kcal/mol relative to experimental ΔG_n° for all n.[88,89]

CCSD and ωB97X-D predictions differ most from experiment, underbinding by up to 8 kcal/mol. As with electronic binding energy predictions, thermochemical results from these two methods compare well with each other. Rao et al.[74] obtained better agreement with experiment by computing the B3LYP/6-311++G** lowest-energy geometry and adding an empirically determined fraction of counterpoise correction for BSSE from MP2 — an approach justified by basis set convergence studies.[76] That approach does not work here since the counterpoise corrections are very small with the aug-cc-pVDZ basis set. We ascribe the shortcomings of the free energy calculations using CCSD either to sensitivity of vibrational frequency analysis to basis set or to a small systematic experimental error.

Energy and enthalpy values are similar for inner- and split-shell structures, suggesting that entropy is the main determinant of split-shell binding. The difficulty in estimating the entropic term has led to disagreement in the literature about the dominant coordination at $T = 298$ K.[6,57,71−74,90] In those works, the level of theory and temperature affect which coordination pattern is the most stable. In contrast, our work indicates that the $n = 4 + 1$ and $n = 4 + 2$ coordinations are the favored structures, even at $T = 0$ K. As the split-shell structures have higher formation entropies, they become even more favorable at elevated temperatures.

4. DISCUSSION

Ions solvated in water clusters are strongly favored over lone ions and lone waters in the vapor phase. Cluster studies can help reveal how solvent builds up around an ion even in aqueous environments.[6,91] Ion clusters are also one of the few sources of experimental data for single-ion properties.[92] Furthermore, isolated clusters are a crucial ingredient in quasi-chemical theory (QCT)[81,85,93,94] and combined quantum mechanics/molecular mechanics (QM/MM) calculations.[95] As an example, $n = 4$ ion−water complexes in gas-phase formed the basis for investigations of alkali metal ion hydration[96] (e.g., Li^+,[82,83] Na^+,[84,97] K^+,[97,98] Rb^+[99]), and other gas-phase complexes underpinned studies of hydration for alkaline earth and transition metals[100,101] and gas molecules.[102−105] Accurate thermochemical predictions of ion hydration[106] are crucial to understanding ion partitioning from water to other solvation environments. Solvation in nonaqueous environments may also be analyzed in a cluster framework, as done in prior studies of ion-binding sites in proteins,[79,107−109] ion carriers,[110] metalloporphyrins,[111] and trapping of gas molecules in clathrates.[112]

While dispersion corrections to density functionals are important in many solvation problems, including pure water hydration in bulk and clusters,[14,113] the need for those corrections in ion hydration has been unclear. DFT already works well for electrostatics.[114] In an ion−water cluster, the dearth of water molecules increases the relative importance of the ion−water interaction, which is primarily electrostatic in nature.[115] In tightly bound ionic systems, the dispersion contribution may be overpowered by screening or other electrostatic effects. In liquid water, dispersion corrections alter the first solvation shell of ions, but these changes lessen agreement with experimental structures.[116]

For the $Na^+·(H_2O)_n$ clusters studied here, dispersion to correct electron correlation and range separation to correct electron delocalization errors individually add favorable contributions to pairwise ion−water interactions (E_{iw}). Pairwise atomic dispersion methods contribute from −0.2 to −2.0 kcal/mol (0.3% to 3% of binding energy) for each ion−water interaction in $n = 4$ clusters, depending on the amount of

DOI: 10.1021/acs.jctc.5b00357
J. Chem. Theory Comput. 2015, 11, 2958−2967

damping included in the dispersion correction.[117] Since the uncorrected DFs already overbind compared to CCSD, addition of dispersion corrections further enhance the disparity with CCSD predictions. The lower ion−water pairwise interaction energy, E_{iw}, produced by range separation compared to uncorrected functionals also enhance the discrepancy with CCSD binding energies. Surprisingly, the increased HF exchange in the ωB97X-D functional − allowed by a combination of the two corrections, electron delocalization (range correction) and electron correlation (dispersion) − leads to less favorable E_{iw}.

Agreement between ΔE_n predicted by ωB97X-D and CCSD(T) is ascribed principally to low electronic polarization produced by both methods. Conversely, the poorer agreement of other DFs with CCSD(T) binding energies is attributed mainly to their tendency to overpolarize electronic distributions in the sodium-water clusters. An additional source of agreement comes from high-order multiwater interactions. Both ωB97X-D and CCSD(T) predict larger unfavorable contributions to binding energy (ΔE_n) from four-body and higher interactions than other DFs. The agreement between ωB97X-D and CCSD was also reported in a study of a metal ion with organic ligands.[118]

A particularly surprising finding is that CCSD/aug-cc-pVDZ binding enthalpies and free energies agree least well with experiment. Experimental values are shifted 4 kcal/mol lower than CCSD for $\Delta H°$ and $\Delta G°$ (n = 1−4). In the coupled-cluster calculations, increasing the basis set size (from aug-cc-pVDZ to aug-cc-pVTZ) lowers the binding energies, while increasing the level of theory (from CCSD to CCSD(T)) raises the binding energies by ∼0.2−0.5 kcal/mol. Therefore, the discrepancy with experiment may be reduced in the complete basis set limit of CCSD(T).

Thermal corrections computed with CCSD are rare since they are so computationally demanding.[119] Clever implementation methods[120] or methods of extrapolation[121] are necessary to make calculation of coupled-cluster frequencies reasonable in terms of CPU time. In another direct calculation of CCSD vibrational frequencies, Weaver et al. also found poor agreement between CCSD and experimental heats of formation of zinc complexes.[122] Further, DFT methods that predicted shorter bond lengths were more accurate compared to experiment. We find a similar trend (see Figure S1). In particular, CAM-B3LYP predicts the shortest sodium-water distance and is the most accurate relative to experiment.

The differences between density functionals can be related to differences in parametrization. CAM-B3LYP is parametrized using only experimental data (see Tables S1 and S2). In contrast, the parametrization of ωB97X-D includes interaction energies from the S22 data set[22] computed with the CCSD method. The ωB97X-D functional has the most extensive parametrization training set (see Table S1) and the largest number of parameters (18 parameters) of the DFs studied here. LC-ωPBE, another strong performer in comparison with experimental enthalpies and free energies (Tables 3 and 4), uses electron and proton affinities for molecules in the G2/97 and G3/99 test sets and energy barriers for atom transfer reactions from the HTBH38 and NHTBH38 test sets.[45] New schemes[123,124] for reducing electron delocalization error may improve the agreement between standard density functionals and CCSD(T) for binding energy in sodium-water clusters.

5. CONCLUSIONS

We investigated whether long-ranged corrections to density functional theory (DFT) for electron correlation (dispersion) and electron delocalization (range separation in the exchange term) errors increase the accuracy of binding free energy calculations for the hydrated sodium ion with one to six waters. We chose this model system because electrostatic interactions dominate in these clusters, yet water−water interactions fall in a distance region critical for describing dispersive effects. We found that neither dispersion nor range separation alone necessarily improves energies or thermochemical predictions over the base functional.

The ωB97X-D dual-corrected functional best matches the CCSD(T) data used to evaluate binding energies. We attribute the agreement to less overpolarization of water dipoles and less charge transfer from water to sodium for wB97X-D compared to other functionals, as well as more accurate multibody interactions. All density functionals predict binding enthalpies that agree well with experiments and binding free energies that lie within a range of ∼15% from experimental values. Free energies depend sensitively on low-frequency vibrational modes characteristic of hindered rotations in ion−water clusters. Thus, exchange-correlation functionals that describe changes in electronic energy for displacements from the minimum energy in these vibrational modes should perform best. The range-separated CAM-B3LYP best matches experimental values for both binding enthalpies and free energies despite relatively large electronic polarization. These results support the use of charged, highly polarized systems containing multiple atoms and systems displaced from minimum-energy geometries alongside traditional noncovalent complexes made of atomic pairs evaluated at lowest-energy geometries for density functional parametrization.

Finally, we assessed the sodium-water coordination pattern with all inner-shell or with split-shell water occupation. The stability of split-shell versus inner-shell coordination structures varies with method, but only the split-shell structures for $n \geq 5$ recover the correct experimental trend for binding free energy.

■ ASSOCIATED CONTENT

Supporting Information

Information on the parametrization and training sets for DF development, geometry information, and binding enthalpies and free energies for aug-cc-pVTZ basis set. The Supporting Information is available free of charge on the ACS Publications website at DOI: 10.1021/acs.jctc.5b00357.

■ AUTHOR INFORMATION

Corresponding Author

*Phone: 505 845-0253 E-mail: slrempe@sandia.gov.

Notes

The authors declare no competing financial interest.

■ ACKNOWLEDGMENTS

M.S. gratefully acknowledges support from the State of Louisiana Board of Regents and the National Science Foundation under the NSF EPSCoR Cooperative Agreement No. EPS-1003897. D.M.R. acknowledges support from the University of South Florida Research Foundation. D.M.R. and S.B.R. acknowledge Sandia's LDRD program. This work was also supported in part by the National Science Foundation under Grant No. PHYS-1066293 and the hospitality of the

DOI: 10.1021/acs.jctc.5b00357
J. Chem. Theory Comput. 2015, 11, 2958−2967

Aspen Center for Physics. Sandia National Laboratories is a multiprogram laboratory managed and operated by Sandia Corporation, a wholly owned subsidiary of Lockheed Martin Corporation, for the U.S. Department of Energy's National Nuclear Security Administration under Contract DE-AC04-94AL8500.

REFERENCES

(1) Hille, B. *Ionic Channels of Excitable Membranes*, 3rd ed.; Sinauer Associates, Inc.: Sunderland, MA, 2001.
(2) Andersen, O. S. *J. Gen. Physiol.* **2011**, *137*, 393−395.
(3) Varma, S.; Rogers, D. M.; Pratt, L. R.; Rempe, S. B. *J. Gen. Physiol.* **2011**, *137*, 479−488.
(4) Liu, S.; Bian, X.; Lockless, S. W. *J. Gen. Physiol.* **2012**, *140*, 671−679.
(5) Kołaski, M.; Zakharenko, A. A.; Karthikeyan, S.; Kim, K. S. *J. Chem. Theory Comput.* **2011**, *7*, 3447−3459.
(6) Lee, H. M.; Tarakeshwar, P.; Park, J.; Kołaski, M. R.; Yoon, Y. J.; Yi, H.-B.; Kim, W. Y.; Kim, K. S. *J. Phys. Chem. A* **2004**, *108*, 2949−2958.
(7) Cohen, A. J.; Mori-Sanchez, P.; Yang, W. *Chem. Rev.* **2012**, *112*, 289−320.
(8) Mattsson, A. E. *Science* **2002**, *298*, 759−760.
(9) Johnson, E. R.; Mackie, I. D.; DiLabio, G. A. *J. Phys. Org. Chem.* **2009**, *22*, 1127−1135.
(10) Stone, A. J. *The Theory of Intermolecular Forces*; Oxford Univerity Press: USA, 1997.
(11) Rempe, S. B.; Mattsson, T. R.; Leung, K. *Phys. Chem. Chem. Phys.* **2008**, *10*, 4685−4687.
(12) Wang, J.; Roman-Perez, G.; Soler, J. M.; Artacho, E.; Fernandez-Serra, M.-V. *J. Chem. Phys.* **2011**, *134*, 024516.
(13) Lin, I.; Seitsonen, A. P.; Tavernelli, I.; Rothlisberger, U. *J. Chem. Theory Comput.* **2012**, *8*, 3902−2910.
(14) Santra, B.; Michaelides, A.; Fuchs, M.; Tkatchenko, A.; Filippi, C.; Scheffler, M. *J. Chem. Phys.* **2008**, *129*, 194111.
(15) Payandeh, J.; Scheuer, T.; Zheng, N.; Catterall, W. A. *Nature* **2011**, *475*, 353−358.
(16) Chai, J.-D.; Head-Gordon, M. *Chem. Phys. Lett.* **2008**, *467*, 176−178.
(17) Kowalski, K.; Hammond, J. R.; de Jong, W. A. *J. Chem. Phys.* **2007**, *127*, 164105.
(18) Cramer, C. J. *Essentials of Computational Chemistry: Theories and Models*, 2nd ed.; John Wiley & Sons, Inc.: West Sussex, England, 2004.
(19) Burke, K. *J. Chem. Phys.* **2012**, *136*, 150901.
(20) Pribram-Jones, A.; Gross, D. A.; Burke, K. *Annu. Rev. Phys. Chem.* **2015**, *66*, 283−304.
(21) Grimme, S. *Wiley Interdiscip. Rev.: Comput. Mol. Sci.* **2011**, *1*, 211−228.
(22) Jurecka, P.; Sponer, J.; Cerny, J.; Hobza, P. *Phys. Chem. Chem. Phys.* **2006**, *8*, 1985−1993.
(23) Varma, S.; Rempe, S. B. *Biophys. J.* **2010**, *99*, 3394−3401.
(24) Mori-Sánchez, P.; Cohen, A. J.; Yang, W. *J. Chem. Phys.* **2006**, *125*, 201102.
(25) Cohen, A. J.; Mori-Sánchez, P.; Yang, W. *J. Chem. Phys.* **2007**, *126*, 191109.
(26) Cohen, A. J.; Mori-Sanchez, P.; Yang, W. *Science* **2008**, *321*, 792.
(27) Mori-Sánchez, P.; Cohen, A. J.; Yang, W. *Phys. Rev. Lett.* **2009**, *102*, 066403.
(28) Rohrdanz, M. A.; Martins, K. M.; Herbert, J. M. *J. Chem. Phys.* **2009**, *130*, 054112.
(29) Yanai, T.; Tew, D. P.; Handy, N. C. *Chem. Phys. Lett.* **2004**, *393*, 51−57.
(30) Lao, K. U.; Herbert, J. M. *J. Chem. Phys.* **2014**, *140*, 044108.
(31) Chai, J.-D.; Head-Gordon, M. *Phys. Chem. Chem. Phys.* **2008**, *10*, 6615−6620.
(32) Lin, Y.-S.; Tsai, C.-W.; Li, G.-D.; Chai, J.-D. *J. Chem. Phys.* **2012**, *136*, 154109.
(33) Lin, Y.-S.; Li, G.-D.; Mao, S.-P.; Chai, J.-D. *J. Chem. Theory Comput.* **2013**, *9*, 263−272.
(34) Becke, A. D. *J. Chem. Phys.* **1993**, *98*, 5648−5652.
(35) Lee, C.; Yang, W.; Parr, R. G. *Phys. Rev. B* **1988**, *37*, 785−789.
(36) Vosko, S. H.; Wilk, L.; Nusair, M. *Can. J. Phys.* **1980**, *58*, 1200−1211.
(37) Stephens, P. J.; Devlin, F. J.; Chabalowski, C. F.; Frisch, M. J. *J. Phys. Chem.* **1994**, *98*, 11623−11627.
(38) Grimme, S. *J. Comput. Chem.* **2006**, *27*, 1787−1799.
(39) Chai, J.-D.; Head-Gordon, M. *J. Chem. Phys.* **2008**, *128*, 084106.
(40) Becke, A. D. *J. Chem. Phys.* **1997**, *107*, 8554−8560.
(41) Schmider, H. L.; Becke, A. D. *J. Chem. Phys.* **1998**, *108*, 9624−9631.
(42) Perdew, J. P.; Burke, K.; Ernzerhof, M. *Phys. Rev. Lett.* **1996**, *77*, 3865.
(43) Perdew, J. P.; Burke, K.; Ernzerhof, M. *Phys. Rev. Lett.* **1997**, *78*, 1396−1396.
(44) Vydrov, O. A.; Heyd, J.; Krukau, A. V.; Scuseria, G. E. *J. Chem. Phys.* **2006**, *125*, 074106.
(45) Vydrov, O. A.; Scuseria, G. E. *J. Chem. Phys.* **2006**, *125*, 234109.
(46) Vydrov, O. A.; Scuseria, G. E.; Perdew, J. P. *J. Chem. Phys.* **2007**, *126*, 154109.
(47) Čížek, J. In *Advances in Chemical Physics*; Hariharan, P. C., Ed.; John Wiley & Sons, Inc.:1969; Vol. *14*, pp 35−89.
(48) Purvis, I.; George, D.; Bartlett, R. J. *J. Chem. Phys.* **1982**, *76*, 1910−1918.
(49) Scuseria, G. E.; Janssen, C. L.; Schaefer, H. F., III *J. Chem. Phys.* **1988**, *89*, 7382−7387.
(50) Scuseria, G. E.; Schaefer, H. F., III *J. Chem. Phys.* **1989**, *90*, 3700−3703.
(51) Krishnan, R.; Binkley, J. S.; Seeger, R.; Pople, J. A. *J. Chem. Phys.* **1980**, *72*, 650−654.
(52) Bader, R. *Atoms in Molecules: A Quantum Theory*; Oxford University Press: New York, 1990.
(53) Lu, T.; Chen, F. *J. Comput. Chem.* **2012**, *33*, 580−592.
(54) Rempe, S. B.; Watts, R. O. *Chem. Phys. Lett.* **1997**, *269*, 455−463.
(55) Rempe, S.; Watts, R. *J. Chem. Phys.* **1998**, *108*, 10084−95.
(56) Ochterski, J. W. *Thermochemistry in Gaussian*; 2002.
(57) Kim, J.; Lee, S.; Cho, S. J.; Mhin, B. J.; Kim, K. S. *J. Chem. Phys.* **1995**, *102*, 839.
(58) Tissandier, M. D.; Cowen, K. A.; Feng, W. Y.; Gundlach, E.; Cohen, M. H.; Earhart, A. D.; Coe, J. V.; Tuttle, T. R., Jr. *J. Phys. Chem. A* **1998**, *102*, 7787−7794.
(59) Kebarle, P. In *Modern Aspects of Electrochemistry*; Conway, B. E., Bockris, J. O., Eds.; Plenum Press: New York, 1974; Vol. *9*.
(60) Lee, N.; Keesee, R. G.; Castleman, A. W., Jr. *Colloid Interface Sci.* **1980**, *75*, 555.
(61) Rempe, S. B.; Jónsson, H. *Chem. Educ.* **1998**, *3*, 04231−04236.
(62) Kathmann, S.; Schenter, G.; Garrett, B. *J. Phys. Chem. C* **2007**, *111*, 4977−4983.
(63) Rogers, D. M.; Rempe, S. B. *J. Phys. Chem. B* **2011**, *115*, 9116−9129.
(64) Glaesemann, K. R.; Fried, L. E. *J. Chem. Phys.* **2005**, *123*, 34103.
(65) McClurg, R. B.; Flagan, R. C.; Goddard, W. A., III *J. Chem. Phys.* **1997**, *106*, 6675.
(66) Ayala, P. Y.; Schlegel, H. B. *J. Chem. Phys.* **1998**, *108*, 2314−25.
(67) Valiev, M.; Bylaska, E. J.; Govind, N.; Kowalski, K.; Straatsma, T. P.; van Dam, H. J. J.; Wang, D.; Nieplocha, J.; Apra, E.; Windus, T. L.; de Jong, W. A. *Comput. Phys. Commun.* **2010**, *181*, 1477.
(68) Schuchardt, K. L.; Didier, B. T.; Elsethagen, T.; Sun, L.; Gurumoorthi, V.; Chase, J.; Li, J.; Windus, T. L. *J. Chem. Inf. Model.* **2007**, *47*, 1045−1052.
(69) Feller, D. *J. Comput. Chem.* **1996**, *17*, 1571−1586.
(70) Frisch, M. J.; Trucks, G. W.; Schlegel, H. B.; Scuseria, G. E.; Robb, M. A.; Cheeseman, J. R.; Scalmani, G.; Barone, V.; Mennucci, B.; Petersson, G. A.; Nakatsuji, H.; Caricato, M.; Li, X.; Hratchian, H. P.; Izmaylov, A. F.; Bloino, J.; Zheng, G.; Sonnenberg, J. L.; Hada, M.; Ehara, M.; Toyota, K.; Fukuda, R.; Hasegawa, J.; Ishida, M.; Nakajima,

DOI: 10.1021/acs.jctc.5b00357
J. Chem. Theory Comput. 2015, 11, 2958−2967

T.; Honda, Y.; Kitao, O.; Nakai, H.; Vreven, T.; Montgomery, J. A., Jr.; Peralta, J. E.; Ogliaro, F.; Bearpark, M.; Heyd, J. J.; Brothers, E.; Kudin, K. N.; Staroverov, V. N.; Kobayashi, R.; Normand, J.; Raghavachari, K.; Rendell, A.; Burant, J. C.; Iyengar, S. S.; Tomasi, J.; Cossi, M.; Rega, N.; Millam, J. M.; Klene, M.; Knox, J. E.; Cross, J. B.; Bakken, V.; Adamo, C.; Jaramillo, J.; Gomperts, R.; Stratmann, R. E.; Yazyev, O.; Austin, A. J.; Cammi, R.; Pomelli, C.; Ochterski, J. W.; Martin, R. L.; Morokuma, K.; Zakrzewski, V. G.; Voth, G. A.; Salvador, P.; Dannenberg, J. J.; Dapprich, S.; Daniels, A. D.; Farkas, O.; Foresman, J. B.; Ortiz, J. V.; Cioslowski, J.; Fox, D. J. *Gaussian 09 Revision A.1*; Gaussian Inc.: Wallingford, CT, 2009.

(71) Feller, D.; Glendening, E. D.; Woon, D. E.; Feyereisen, M. W. *J. Chem. Phys.* **1995**, *103*, 3526.

(72) Mitani, M.; Yoshioka, Y. *J. Mol. Struct.: THEOCHEM* **2009**, *915*, 160−169.

(73) Miller, D. J.; Lisy, J. M. *J. Am. Chem. Soc.* **2008**, *130*, 15393−15404.

(74) Rao, J. S.; Dinadayalane, T. C.; Leszczynski, J.; Sastry, G. N. *J. Phys. Chem. A* **2008**, *112*, 12944−12953.

(75) Haunschild, R.; Henderson, T. M.; Jiménez-Hoyos, C. A.; Scuseria, G. E. *J. Chem. Phys.* **2010**, *133*, 134116.

(76) Richard, R. M.; Lao, K. U.; Herbert, J. M. *J. Chem. Phys.* **2013**, *139*, 224102.

(77) Krekeler, C.; Delle Site, L. *J. Phys.: Condens. Matter* **2007**, *19*, 192101.

(78) Dahlke, E. E.; Truhlar, D. J. *J. Phys. Chem. B* **2006**, *110*, 10595−10601.

(79) Rossi, M.; Tkatchenko, A.; Rempe, S. B.; Varma, S. *Proc. Nat. Acad. Sci.* **2013**, *110*, 12978−83.

(80) Grimme, S. DFT-D3. http://www.thch.uni-bonn.de/tc/index.php?section/downloads&subsection/getd3&lang/english (accessed June 1, 2015).

(81) Pratt, L. R.; Rempe, S. B. In *Simulation and Theory of Electrostatic Interactions in Solution*; Hummer, G., Pratt, L. R., Eds.; AIP Press: New York, Vol. *492*, 1999; pp 177−201.

(82) Rempe, S. B.; Pratt, L. R.; Hummer, G.; Kress, J. D.; Martin, R. L.; Redondo, A. *J. Am. Chem. Soc.* **2000**, *122*, 966.

(83) Alam, T.; Hart, D.; Rempe, S. *Phys. Chem. Chem. Phys.* **2011**, *13*, 13629.

(84) Rempe, S. B.; Pratt, L. R. *Fluid Phase Equilib.* **2001**, *183−184*, 121−132.

(85) Rogers, D. M.; Jiao, D.; Pratt, L. R.; Rempe, S. B. In *Annual Reports in Computational Chemistry*; Wheeler, R., Ed.; Elsevier: 2012; Vol. *8*, Chapter 4, pp 71−127.

(86) Džidić, I.; Kebarle, P. *J. Phys. Chem.* **1970**, *74*, 1466−1474.

(87) Jimenez-Hoyos, C. A.; Janesko, B. G.; Scuseria, G. E. *Phys. Chem. Chem. Phys.* **2008**, *10*, 6621−6629.

(88) Feller, D.; Peterson, K. A. *J. Chem. Phys.* **2007**, *126*, 114105.

(89) DiStasio, R. A.; von Lilienfeld, O. A.; Tkatchenko, A. *Proc. Natl. Acad. Sci. U. S. A.* **2012**, *109*, 14791−14795.

(90) Patwari, G. N.; Lisy, J. M. *J. Chem. Phys.* **2003**, *118*, 8555.

(91) Chandrasekhar, J.; Spellmeyer, D. C.; Jorgensen, W. L. *J. Am. Chem. Soc.* **1984**, *106*, 903−910.

(92) Herce, D. H.; Perera, L.; Darden, T. A.; Sagui, C. *J. Chem. Phys.* **2005**, *122*, 024513.

(93) Beck, T.; Paulaitis, M. E.; Pratt, L. R. *The potential distribution theorem and models of molecular solutions*; Cambridge University Press: New York, 2006.

(94) Asthagiri, D.; Dixit, P. D.; Merchant, S.; Paulaitis, M. E.; Pratt, L. R.; Rempe, S. B.; Varma, S. *Chem. Phys. Lett.* **2010**, *485*, 1−7.

(95) Friesner, R. A.; Guallar, V. *Annu. Rev. Phys. Chem.* **2005**, *56*, 389−427.

(96) Varma, S.; Rempe, S. B. *Biophys. Chem.* **2006**, *124*, 192−199.

(97) Varma, S.; Rempe, S. B. *J. Am. Chem. Soc.* **2008**, *130*, 15405−15419.

(98) Rempe, S. B.; Asthagiri, D.; Pratt, L. R. *Phys. Chem. Chem. Phys.* **2004**, *6*, 1966.

(99) Sabo, D.; Jiao, D.; Varma, S.; Pratt, L. R.; Rempe, S. B. *Annu. Rep. Prog. Chem., Sect. C: Phys. Chem.* **2013**, *109*, 266.

(100) Asthagiri, D.; Pratt, L. R.; Paulaitis, M.; Rempe, S. B. *J. Am. Chem. Soc.* **2004**, *126*, 1285−1289.

(101) Jiao, D.; Leung, K.; Rempe, S. B.; Nenoff, T. M. *J. Chem. Theory Comput.* **2011**, *7*, 485−495.

(102) Ashbaugh, H. S.; Asthagiri, D.; Pratt, L. R.; Rempe, S. B. *Biophys. Chem.* **2003**, *105*, 323−338.

(103) Sabo, D.; Rempe, S.; Greathouse, J.; Martin, M. G. *Mol. Sim.* **2006**, *32*, 269−278.

(104) Sabo, D.; Varma, S.; Martin, M. G.; Rempe, S. B. *J. Phys. Chem. B* **2008**, *112*, 867−876.

(105) Jiao, D.; Rempe, S. B. *J. Chem. Phys.* **2011**, *134*, 224506.

(106) Leung, K.; Rempe, S. B.; von Lilienfeld, O. A. *J. Chem. Phys.* **2009**, *130*, 204507.

(107) Varma, S.; Rempe, S. B. *Biophys. J.* **2007**, *93*, 1093−1099.

(108) Dudev, T.; Lim, C. *J. Am. Chem. Soc.* **2009**, *131*, 8092−8101.

(109) Jiao, D.; Rempe, S. B. *Biochemistry* **2012**, *51*, 5979−5989.

(110) Varma, S.; Sabo, D.; Rempe, S. B. *J. Mol. Biol.* **2008**, *376*, 13−22.

(111) Leung, K.; Rempe, S. B.; Schultz, P. A.; Sproviero, E. M.; Batista, V. S.; Chandross, M. E.; Medforth, C. J. *J. Am. Chem. Soc.* **2006**, *128*, 3659−68.

(112) Clawson, J.; Leung, K.; Cygan, R. T.; Alam, T. M.; Rempe, S. B. *J. Comput. Theor. Nanosci.* **2010**, *7*, 2602−06.

(113) Schmidt, J.; VandeVondele, J.; Kuo, I.-F. W.; Sebastiani, D.; Siepmann, J. I.; Hutter, J.; Mundy, C. J. J. *Phys. Chem. B* **2009**, *113*, 11959−11964. PMID: 19663399.

(114) Klimes, J.; Michaelides, A. *J. Chem. Phys.* **2012**, *137*, 120901.

(115) Charles, W.; Bauschlicher, J.; Langhoff, S. R.; Partridge, H.; Rice, J. E.; Komornicki, A. *J. Chem. Phys.* **1991**, *95*, 5142−5148.

(116) Bankura, A.; Carnevale, V.; Klein, M. L. *J. Chem. Phys.* **2013**, *138*, 014501.

(117) Grimme, S.; Antony, J.; Ehrlich, S.; Krieg, H. *J. Chem. Phys.* **2010**, *132*, 154104.

(118) Chen, M.; Craciun, R.; Hoffman, N.; Dixon, D. A. *Inorg. Chem.* **2012**, *51*, 13195−13203.

(119) Miliordos, E.; Apra, E.; Xantheas, S. S. *J. Chem. Phys.* **2013**, *139*, 114302.

(120) Yoo, S.; Aprà, E.; Zeng, X. C.; Xantheas, S. S. *J. Phys. Chem. Lett.* **2010**, *1*, 3122−3127.

(121) Howard, J. C.; Tschumper, G. S. *J. Chem. Phys.* **2013**, *139*, 184113.

(122) Weaver, M. N.; Merz, K. M.; Ma, D.; Kim, H. J.; Gagliardi, L. *J. Chem. Theory Comput.* **2013**, *9*, 5277−85.

(123) Kim, M.-C.; Sim, E.; Burke, K. *J. Chem. Phys.* **2014**, *140*, 18A528.

(124) Li, C.; Zheng, X.; Cohen, A. J.; Mori-Sánchez, P.; Yang, W. *Phys. Rev. Lett.* **2015**, *114*, 053001.

DOI: 10.1021/acs.jctc.5b00357
J. Chem. Theory Comput. 2015, 11, 2958−2967